The current issue and full text archive of this journal is available at
www.emeraldinsight.com/0961-5539.htm

Heat transfer enhancement in turbulent tube flow using Al_2O_3 nanoparticle suspension

Sidi El Bécaye Maïga and Cong Tam Nguyen
Faculty of Engineering, Université de Moncton, Moncton, Canada
Nicolas Galanis
Department of Mechanical Engineering, Faculty of Engineering, Université de Sherbrooke, Sherbrooke, Canada
Gilles Roy
Faculty of Engineering, Université de Moncton, Moncton, Canada, and
Thierry Maré and Mickaël Coqueux
LGCGM INSA de Rennes/IUT de Saint Malo, Saint-Malo, France

Received March 2005
Revised August 2005
Accepted September 2005

Abstract

Purpose – To study the hydrodynamic and thermal behaviors of a turbulent flow of nanofluids, which are composed of saturated water and Al_2O_3 nanoparticles at various concentrations, flowing inside a tube submitted to a uniform wall heat flux boundary condition.

Design/methodology/approach – A numerical method based on the "control-volume" approach was used to solve the system of non-linear and coupled governing equations. The classical κ-ε model was employed in order to model the turbulence, together with staggered non-uniform grid system. The computer model, satisfactorily validated, was used to perform an extended parametric study covering wide ranges of the governing parameters. Information regarding the hydrodynamic and thermal behaviors of nanofluid flow are presented.

Findings – Numerical results show that the inclusion of nanoparticles into the base fluid has produced an augmentation of the heat transfer coefficient, which has been found to increase appreciably with an increase of particles volume concentration. Such beneficial effect appears to be more pronounced for flows with moderate to high Reynolds number. In reverse, the presence of nanoparticles has induced a rather drastic effect on the wall shear stress that has also been found to increase with the particle loading. A new correlation, $Nu_{fd} = 0.085\ Re^{0.71}\ Pr^{0.35}$, is proposed to calculate the fully-developed heat transfer coefficient for the nanofluid considered.

Practical implications – This study has provided an interesting insight into the nanofluid thermal behaviors in the context of a confined tube flow. The results found can be easily exploited for various practical heat transfer and thermal applications.

Originality/value – The present study is believed to be an interesting and original contribution to the knowledge of the nanofluid thermal behaviors.

Keywords Turbulence, Convection, Heat transfer, Nanotechnology, Numerical flexibility

Paper type Research paper

The authors wish to thank the Natural Sciences and Engineering Research Council of Canada, the Faculty of the Graduate Studies and Research of the Université de Moncton for their financial support to the present research project. Thanks are also due to the Faculty of Engineering of the Université de Moncton for allocating the computing facilities.

International Journal of Numerical Methods for Heat & Fluid Flow
Vol. 16 No. 3, 2006
pp. 275-292

0961-5539
DOI 10.1108/09615530610649717

Nomenclature

C_p = specific heat of fluid
D = tube inside diameter
h_{fd} = fully developed heat transfer coefficient
h_Z = local wall heat transfer coefficient
h_r = nanofluid-to-base fluid heat transfer coefficient ratio
I_0 = turbulent intensity at tube inlet
k = fluid thermal conductivity
L = tube length
Nu_{fd} = fully developed Nusselt number, $Nu_{fd} = h_{fd}D/k_0$
Nu_Z = local Nusselt number, $Nu_Z = h_ZD/k_0$
P = pressure
Pr = Prandtl number, $Pr = C_p\mu/k$
q_W'' = imposed uniform wall heat flux
Re = Reynolds number, $Re = \rho_0 V_0 D/\mu_0$
R_0 = tube radius, $R_0 = D/2$
R = radial coordinate
T, t = mean and fluctuating temperature
T_W = fluid temperature at the tube wall
T_0 = fluid inlet temperature (reference temperature)
Z = axial coordinate
$\overline{V}, v$ = mean and fluctuating velocity vector
V_Z = axial velocity component

Greek letters

α = fluid thermal diffusivity
φ = volume concentration of nanoparticles
μ = fluid dynamic viscosity
θ = tangential coordinate
ρ = fluid density

Subscripts

b = bulk condition
bf = base fluid
nf = nanofluid
fd = fully developed condition
p = particles
r = nanofluid-to-base fluid ratio
W = wall condition
Z = axial coordinate
0 = reference (inlet) condition

1. Introduction

Conventional heat transfer fluids such as water, ethylene glycol and engine oil, possess limited capabilities in term of thermal properties while compared to most solids, in particular metals. In spite of considerable research and efforts deployed in the past, a clear need does exist to date regarding the development of new strategies in order to improve the thermal performance of heat transfer equipments. In recent years, modern technologies have permitted the manufacturing of metallic particles down to the nanometer scale, which in turn, has created a new and rather special class of fluids, called nanofluids. The latter refer to two-phase mixtures usually composed of a saturated liquid and a dispersed phase constituted of very fine metallic particles of size below 40 nm, called nanoparticles. It has been known that the thermal properties of such a nanofluid are well higher than those of the base fluid. In fact, some scarce experimental data – see in particular Masuda *et al.* (1993), Choi (1995) and Lee *et al.* (1999) – have clearly shown that with a relatively low particle loading, say from 1 to 5 percent in volume, a 20 percent increase of the apparent thermal conductivity has been noticed for some particle suspensions. Such an increase appears to be dependent on several factors such as particle form and size, its concentration as well as thermal properties of constituents. These nanofluids can then be an interesting alternative for advanced thermal applications, in particular micro and nano scale heat transfer where high heat flux is required (Lee and Choi, 1996).

In spite of their potentials and features, these special fluids are still in their development stage. The very first and rather scarce experimental works were concerned only with the measurement of nanofluids effective thermal conductivity and dynamic viscosity (Masuda *et al.*, 1993; Choi, 1995; Pak and Cho, 1998; Lee *et al.*, 1999;

Wang *et al.*, 1999; Eastman *et al.*, 1999; Xuan and Li, 2000; Eastman *et al.*, 2001). It should be mentioned that in these works, physical and thermal properties of nanofluids were provided for fixed reference temperature, say the ambient temperature. In their recent works, Wang *et al.* (2003) and Xuan *et al.* (2003), employing fractal models, have investigated the effects due to particle clustering on the effective thermal conductivity. Das *et al.* (2003) and Putra *et al.* (2003) were likely the firsts who investigated the influence of temperature on the nanofluid thermal properties. Their measures obtained for water-Al_2O_3 mixture, although being limited to two specific particle volume concentrations, say 1 and 4 percent, have clearly shown that with a temperature increase, the effective thermal conductivity augments considerably; on the other hand, the nanofluid dynamic viscosity decreases appreciably, which appears rather interesting regarding potential uses of nanofluids in thermal applications. It is important to note that, with regard to the nanofluid thermal properties, the actual amount of experimental data available in the literature remains, surprisingly, quite limited. Also, the influence of the particle shape on such properties has yet been clearly understood to date. It is obvious that more research works will be needed in this interesting issue in the near future.

From the theoretical viewpoint, such a liquid and ultra-fine particle mixture represents a new, very interesting yet rather challenging problem to researchers in fluid mechanics and heat transfer. In fact, it appears very difficult to establish any theory that can reasonably predict the flow of nanofluid by considering it as a multi-component fluid (Drew and Passman, 1999). Also, since a nanofluid, by nature, is a two-phase fluid, one can then expect that it may possess common features with the solid-fluid mixtures. On this issue, the question regarding whether the theory of two-phase flows can be applied to nanofluids remains highly questionable. On the other hand, due to particles random movement within the liquid as well as to their extremely reduced size, one should mention some fascinating yet rather complex phenomena such as thermal dispersion, intermolecular energy exchange and liquid layering on the solid-liquid interface as well as phonon effects on the heat transport inside the solid particle itself. Such phenomena are under intensive investigations from researchers around the world, see in particular Keblinski *et al.* (2002) and Ohara and Suzuki (2000).

Regarding the hydrodynamic and thermal behaviors of nanofluid in confined flows, the experimental works by Pak and Cho (1998) and Li and Xuan (2002) have provided interesting insight into thermal performance of nanofluids. In fact, the first empirical correlations were proposed for computing the Nusselt number in both laminar and turbulent tube flow using data collected from nanofluids composed of water and Cu, TiO_2 and γAl_2O_3 particles. Recently, Wen and Ding (2004) have experimentally studied the thermal performance of water-γAl_2O_3 mixture under laminar flow regime in the entrance region of a horizontal heated tube. In their most recent work, Yang *et al.* (2005) have measured the convective heat transfer coefficients of several nanofluids that are composed of graphitic nanoparticles and automatic transmission fluid. Results from these pioneer works have clearly shown that the inclusion of dispersed particles produces a remarkable increase the heat transfer of the base fluid, and the nanofluids considered give, in general, higher heat transfer coefficient than the base-fluid (saturated water) for given Reynolds number. Such improvement becomes more important with an augmentation of the particle loading. Numerical results from the

authors' recent studies (Maïga *et al.*, 2004; Roy *et al.*, 2004) have also confirmed the above beneficial effects due to nanofluids, namely water-γAl_2O_3 and ethylene-γAl_2O_3 mixtures, for two different confined laminar flow configurations. In the present work, we have thoroughly investigated the heat transfer enhancement capability of water-γAl_2O_3 mixture flowing under turbulent regime inside a uniformly heated tube.

2. Mathematical modeling and numerical method

2.1 Governing equations

The problem under consideration consists of steady, forced turbulent convection flow and heat transfer of a nanofluid flowing inside a straight tube of circular cross-section. The fluid possesses uniform temperature and axial velocity profiles at the inlet section. The tube is long enough so that the fully developed flow conditions prevail at the outlet section. Also, the flow and the thermal field are assumed symmetrical with respect to the vertical plane passing through the main axis (Figure 1).

2.1.1 Assumptions. As stated before, it appears that there exists no formulated theory known to date that could reasonably predict the flow behaviors of a nanofluid by considering it as a multi-component material. It is interesting to note that most nanofluids used in practical applications are usually composed of oxide particles finer than 40 nm. Therefore, it has been suggested that the particles may be easily fluidized and consequently, can be considered to behave more like a fluid than a heterogeneous mixture (Xuan and Roetzel, 2000). Furthermore, by assuming negligible motion slip as well as the thermal equilibrium between the phases, the resulting mixture may then be considered as a conventional single-phase fluid, which possesses effective physical properties being function of the properties of both constituents and their respective concentrations (Pak and Cho, 1998; Xuan and Roetzel, 2000). As a result, a direct extension from a conventional fluid to a nanofluid appears feasible, and one may then expect that the classical theory developed for a conventional single-phase fluid can be applied to a nanofluid as well. Thus, all the equations of conservation (mass, momentum and energy) as well known for single-phase fluids can be directly applied to nanofluids.

The above single-phase fluid assumption, which appears somewhat too simplistic, has its own merit and, of course, limit. Owing to a striking lack of data permitting to establish a clear picture of the physical mechanisms governing the suspended nanoparticles within a continuous liquid phase, it appears rather difficult to assess the exact limit of such an important assumption. It is believed that, under the conditions of negligible slip and thermal equilibrium between the phases, and as long as the particle

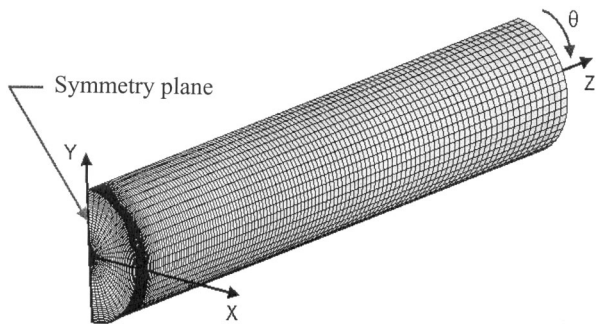

Figure 1.
Geometrical configuration of the problems studied

suspension is assured and their spatial distribution can approximately be considered as uniform throughout the domain, then the single-phase fluid assumption may reasonably be applied. From the practical point of view, one must strictly consider mixtures with relatively low particle concentration; on the other hand, the preparation of such particle-liquid mixture itself must be carefully handled in order to ensure a perfect mixing of the particles inside the liquid phase. It should be noted, as pointed out by Keblinski *et al.* (2005), that the stability of the particle suspension is indeed one of the crucial issues for both scientific research and practical applications.

It is very interesting to mention that, although more experimental data will be needed in order to assess the single-phase fluid assumption, it seems to be validated, to some extent, through the experimental results by Pak and Cho (1998) and Li and Xuan (2002) in which correlations of a form similar to that of the well-known Dittus-Boelter formula were proposed to characterize nanofluids heat transfer. Such a validation also appears to be held as well through the satisfactory comparisons of our numerical results presented later in this paper.

In this work, we have adopted the above "single phase fluid" approach in order to be able to studying the thermal behaviors of nanofluids. Also, the water-γAl_2O_3 mixture under consideration is assumed incompressible with constant physical properties which are to be evaluated for a given particle concentration and at the reference state corresponding to the fluid inlet temperature. Under such conditions, the general conservation equations written in the vector form are as follows (Warsi, 1999; Yuan, 1967):

$$\mathrm{div}(\rho \overline{V}) = 0 \tag{1}$$

$$\mathrm{div}(\rho \overline{V}\,\overline{V}) = -\mathrm{grad}(\overline{P}) + \mu \nabla^2 \overline{V} - \mathrm{div}(\rho \bar{v}\bar{v}) \tag{2}$$

$$\mathrm{div}(\rho \overline{V} C_p T) = \mathrm{div}(k\,\mathrm{grad}\,T - \rho C_p \bar{v}\bar{t}) \tag{3}$$

In the above equations, symbols in upper case such as $\bar{v}$, P and T represent the time averaged variables, while those in lower case such as v and t stand for the fluctuating part of the variables considered; the terms $\rho\bar{v}\bar{v}$ and $\rho C_p \bar{v}\bar{t}$ represent, in fact, the Reynolds stresses tensor and the turbulent heat fluxes that are unknown and must be appropriately determined in term of the mean velocity and temperature fields corresponding to the problem under consideration.

2.1.2 Modeling of turbulence. For the proper closing of the governing equations (2) and (3), one needs to introduce empirical data or approximate models to express the turbulent stresses and heat-flux quantities to the related physical phenomenon. In the present study, we have adopted the well-known and classical κ-ε turbulent model as proposed by Launder and Spalding (1974), which introduces two additional equations of conservation, namely the equation of the turbulent kinetic energy, κ, and the corresponding one for the rate of dissipation, ε. The simplifying form of these equations is given as follows in the divergence-gradient form:

$$\mathrm{div}(\rho \bar{V} \kappa) = \mathrm{div}\{(\mu + \mu_t/\sigma_\kappa)\,\mathrm{grad}\,\kappa)\} + G_\kappa - \rho\varepsilon \tag{4}$$

$$\mathrm{div}(\rho \bar{V} \varepsilon) = \mathrm{div}\{(\mu + \mu_t/\sigma_\varepsilon)\,\mathrm{grad}\,\varepsilon)\} + C_{1\varepsilon}(\varepsilon/\kappa)G_\kappa + C_{2\varepsilon}\rho(\varepsilon^2/\kappa) \tag{5}$$

In the above equations, G_κ represents the generation of turbulence kinetic energy due to the mean velocity gradients; $C_{1\varepsilon}$ and $C_{2\varepsilon}$ are constant; σ_κ and σ_ε are the turbulent

Prandtl numbers for κ and ε, respectively; and μ_t is the turbulent (or eddy) viscosity, computed as:

$$\mu_t = \rho C_\mu \kappa^2 / \varepsilon \tag{6}$$

where C_μ is a constant.

The various constant of the κ-ε model are given as follows (Launder and Spalding, 1974; Anderson *et al.*, 1984):

$$C_{1\varepsilon} = 1.44; \quad C_{2\varepsilon} = 1.92; \quad C_\mu = 0.09; \quad \sigma_\kappa = 1.0 \quad \text{and} \quad \sigma_\varepsilon = 1.3 \tag{7}$$

Note that the complete details regarding the derivation of the Reynolds form of the conservation equations as well as the κ-ε turbulent model have been very well documented elsewhere (the reader is invited to consult, in particular, the above named references for further details). Regarding the turbulent viscosity μ_t in particular, there is, unfortunately, a clear lack of data permitting an appropriate quantification of this property for use with mixtures containing nanoparticles. Since we have assumed that the nanofluid would behave as a single-phase homogenous fluid, the turbulent viscosity μ_t may then be evaluated as for a conventional fluid, says by the equation (6) according to the κ-ε turbulent model. Furthermore, it is important to mention that, although there are several others semi-empirical turbulent models that can be employed for the tube flow, their performance for use in the case of nanofluid flows has yet been established. We have adopted the κ-ε model mainly because of its simplicity. As we can notice later in Section 3.2 where a successful comparison has been carried out against empirical correlations for turbulent flow, the κ-ε model appears, to our opinion, to perform quite satisfactorily with nanofluids.

2.2 Boundary conditions

The conservation equations (1)-(5) constitute a non-linear and highly coupled PDE system that must be appropriately solved subject to the following boundary conditions. At the tube inlet section, uniform profiles of fluid axial velocity V_0, temperature T_0 and turbulent intensity I_0 have been prescribed; by assuming turbulence isotropy, the turbulent kinetic energy at the inlet section can then be evaluated as $\kappa_0 = 1.5 I_0^2 V_0^2$ (Warsi, 1999). At the outlet section, the fully developed conditions prevail, that is to say that all axial derivatives are zero. On the tube wall, the usual non-slip conditions are imposed, all velocity components and turbulent parameters such as κ and ε are zero; also, the condition of uniform wall heat flux prevails. In this study, the treatments of the near-wall region were based on the classical and well-known wall functions as proposed by Launder and Spalding (1974), see also Launder and Spalding (1972) and Warsi (1999) for complete details. Finally, it has been assumed that both the flow and thermal fields are symmetrical with respect to the vertical plane passing through the tube longitudinal main axis.

2.3 Thermal and physical properties of nanofluids

By assuming that the particles are well dispersed within the base-fluid, i.e. the particle concentration may be considered as uniform throughout the domain, the effective thermal properties of the nanofluid studied can be evaluated by using the following classical relations developed for a two-phase mixture (indices "p", "bf" and "nf" refer, respectively, to the particles, the base-fluid and the nanofluid, while "r" refers to the "nanofluid/base fluid" ratio of the physical quantity under consideration):

$$\rho_{nf} = (1 - \varphi)\rho_{bf} + \varphi\rho_p \quad (8)$$

$$(C_p)_{nf} = (1 - \varphi)(C_p)_{bf} + \varphi(C_p)_p \quad (9)$$

$$\mu_r = \frac{\mu_{nf}}{\mu_{bf}} = 123\varphi^2 + 7.3\varphi + 1 \quad (10)$$

$$k_r = \frac{k_{nf}}{k_{bf}} = 4.97\varphi^2 + 2.72\varphi + 1 \quad (11)$$

The equations (8) and (9) are general relationships usually used to compute the density and specific heat for a classical two-phase mixture (Pak and Cho, 1998). For the dynamic viscosity of the nanofluid studied, equation (10) has been introduced to compute the dynamic viscosity of water-γAl_2O_3 mixture. Such an equation was obtained by performing a least-square curve fitting from Wang *et al.* (1999) experimental data. With regard to its effective thermal conductivity over the desired range of particle concentration (say up to 10 percent), we have introduced the equation (11) that was obtained based on the empirical model proposed by Hamilton and Crosser (1962) assuming spherical shape of particles. It is very interesting to note that this model, although being originally developed based on data collected from mixtures containing millimeter and micrometer size particles, appears appropriate for nanoparticles (Xuan and Roetzel, 2000). Details and discussion regarding the determination of the thermal properties of the nanofluid studied, in particular the equations (10) and (11), have been presented elsewhere (Maïga *et al.*, 2004; Maïga, 2004) and hence, are not repeated in this paper for the sake of space.

2.4 Dimensionless governing parameters

One can determine that the problem under consideration is characterized by a set of five dimensionless parameters, namely the flow Reynolds number *Re*, the Prandtl number *Pr*, the particle volume concentration φ and the property ratios k_p/k_{bf} and $(C_p)_p/(C_p)_{bf}$, their definition is given in the Nomenclature. It should be noted that the shape and dimension of particles themselves also constitute factors that may have important effect on the heat transfer and fluid flow characteristics of nanofluids as well. Such an influence, unfortunately, has yet to be clearly determined to date.

2.5 Numerical method and code validation

The system of governing equations (1)-(5) was solved by employing the "finite control volume" numerical method. Since such method has been very well documented elsewhere, only a brief review is given here. This method is essentially based on the spatial integration of conservation equations over finite control volumes, using the well known power-law scheme to compute the so-called "combined convection-and-diffusion" fluxes of heat, momentum and other quantities resulting from the transport process. Also, the staggered grids have been used where the velocity components are calculated at the center of the volume interfaces while the pressure as well as other scalar quantities such as temperature and turbulent variables κ and ε, for example, are computed at the center of the control volume itself. The algebraic "discretized equations" resulting from the integration process were sequentially, i.e. one at a time, and iteratively

solved throughout the physical domain considered, by combining the "line-by-line" procedure, the three diagonal matrix algorithm technique and the efficient alternate-direction and multi-passes-sweeping technique. On the other hand, the special "pressure-correction" equation, obtained by a combination of the discretized form of the Navier-Stokes equation (2) and the corresponding one of the continuity equation (1), has been employed not only to calculate the guessed pressure field, but also to correct the guessed velocities field in order to progressively satisfy all the discretized equations (the reader is advised to consult Patankar (1980) for complete details regarding the numerical method and procedures).

In order to ensure not only the accuracy of numerical results but also their independence with respect to the number of grid points employed, several non-uniform grids were extensively probed through a rigorous procedure (Maïga, 2004; Maïga *et al.*, 2004), which has shown that the $32 \times 24 \times 155$ non-uniform grid appears satisfactory for the tube flow problem under consideration. This grid possesses 32, 24 and 155 nodes, respectively, along the radial, tangential (for θ varying from 0 to 180°) and axial directions, with highly packed grid points near the tube wall and in particular, in the entrance region of the tube; while the angular increment is constant along the tangential direction. As convergence indicator, we have considered the residuals that result from the integration of conservation equations (1)-(5) over finite control-volumes. During the calculation process, these residuals were constantly monitored and scrutinized; for the simulations performed in this study, converged solutions were usually achieved with residuals as low as 10^{-8} (at least) for all of the governing equations.

The computer model has been successfully validated for both laminar and turbulent flow regimes (Maïga *et al.*, 2004; Maïga, 2004). With regard to the turbulent tube flow which is under consideration, Figure 2(a) shows, for example, the numerical results for the mean axial velocity profile as obtained for various Reynolds number. For comparison purpose, the well known theoretical Blasius 1/7th and 1/10th velocity distributions as well as some experimental data by Nikuradse (Yuan, 1967) are also shown. The concordance with the above data may be qualified as satisfactory although our values of *Re* are unfortunately different. Figure 2(b) shows another comparison for the Nusselt number as function of the flow parameter *Re*. Again, the agreement between our results and the well known Dittus and Boelter (1930) correlation appears quite acceptable except for the case $Re = 10{,}000$ where a relatively important discrepancy has been noticed. Such behavior, after further testing and investigation, is believed to be due to the fact that the κ-ε model could not adequately predict behaviors of a low Reynolds number turbulent flow.

In light of the above satisfactory validation tests, one can conclude with confidence about the appropriateness of the mathematical model as well as the reliability of the numerical method adopted in this study.

3. Results and discussion

The numerical simulations have been carried out for water-γAl_2O_3 mixture and various particle concentrations φ varying from 0 to 10 percent. The tube has a diameter of 0.01 and 1 m of length. The fluid inlet temperature has been fixed to 293.15 K and the flow Reynolds number has varied from 10^4 to 5×10^5. In the following, some

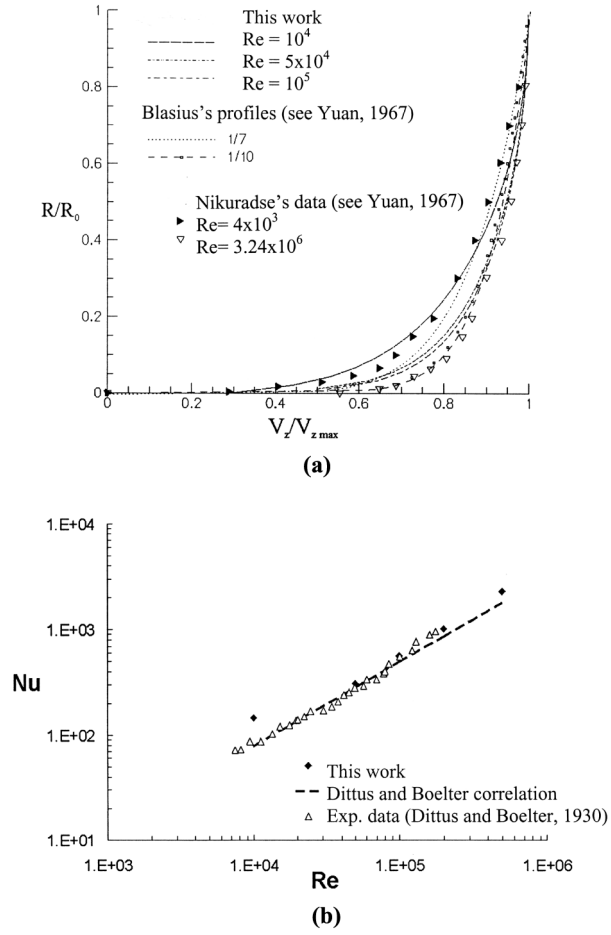

Figure 2.
Results from validation tests: (a) fully developed axial velocity profiles; and (b) fully developed Nusselt number as function of *Re*

significant results showing the beneficial effects due to the presence of nanoparticles are presented and discussed.

3.1 Effect of nanoparticles on axial development of the thermal field

Figure 3(a) shows, at first, the axial development of fluid bulk and wall temperatures as function of particle loading parameter φ for the particular case $Re = 10^5$ with a wall heat flux of $q_W'' = 5 \times 10^5\ \mathrm{W/m^2}$. One can observe that with the increase of φ, both temperatures have clearly and appreciably decreased. Such a diminution is observed all along the tube length, and is more pronounced towards the tube end. Thus, at the outlet section, for example, a decrease of nearly 10 K is achieved for φ increasing from 0 (i.e. base fluid) to 10 percent. Such a beneficial effect can be attributed, in major part, to the fact that with the increase of particle loading, the resulting mixture thermal properties become greatly improved. Thus, for the case $\varphi = 10$ percent, for example, values of its heat capacity ρC_p and thermal conductivity k have majored by nearly 18 and 32 percent with respect to those of the base fluid. The same beneficial influence due

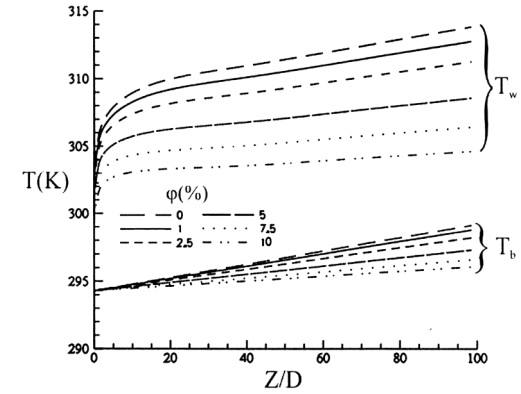

(a)

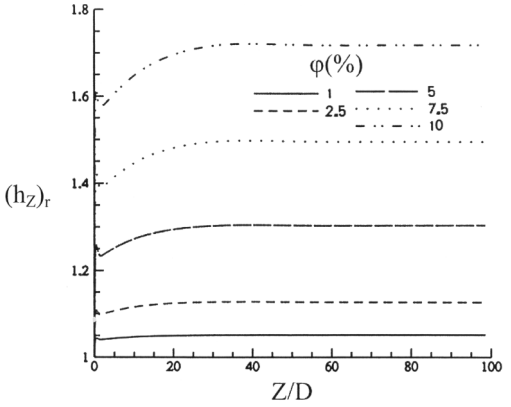

(b)

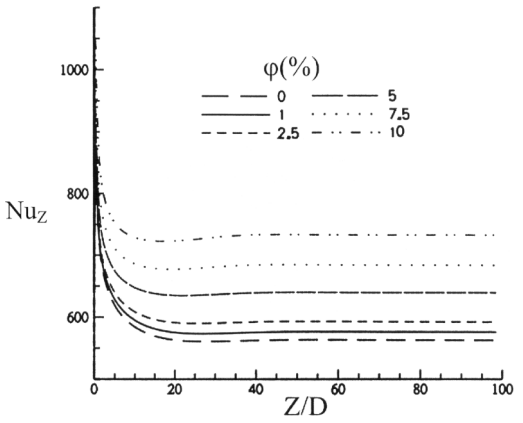

(c)

Figure 3.
For case $Re = 10^5$, effect of φ on axial development of: (a) fluid bulk and wall temperatures; (b) local heat transfer coefficient ratio; and (c) local Nusselt number

to the inclusion of nanoparticles has been consistently observed for other Reynolds numbers considered in this study. It is also interesting to notice a rapid axial development of wall temperature in the entrance region of the tube, behavior that appears physically realistic for a turbulent tube flow (Yuan, 1967).

The above beneficial effect due to nanoparticles may be better observed on Figure 3(b), which shows, for the same cases considered, the axial development of the local heat transfer coefficient ratio $(h_Z)_r$ – defined as $(h_Z)_r = (h_Z)_{nf}/(h_Z)_{bf}$ – as function of the parameter φ. It is clearly observed that the latter has a tremendous influence on the heat transfer rate. Thus, for the case $\varphi = 10$ percent and $Re = 10^5$, for example, one can see that the heat transfer augmentation of nearly 72 percent is achieved at the tube end while compared to the base fluid at same Reynolds number. It is also observed that the ratio h_r increases steeply in the entrance region and reaches a constant value at a short distance, say within 40 diameters from the tube inlet. Such behavior, which has not been observed in the case of laminar flow of nanofluids (Maïga *et al.*, 2004), is clearly a characteristic of turbulent flow where the axial development of the hydrodynamic and thermal fields is generally more accelerated than that of a laminar one.

Figure 3(c) shows the axial variation of the local Nusselt number for the cases considered earlier. It is interesting to observe that in the vicinity of the inlet section, say within few diameters, very high values of the Nusselt number, and hence of the local heat transfer coefficient, can be achieved under the combined effect due to nanoparticles and boundary layer development. Here again, one can observe that, in general, the Nusselt number increases considerably with an augmentation of particle loading. Thus, for example, for the case shown, Nu_Z near the tube exit has increased from 563 to 732 for φ varying from 0 to 10 percent, an augmentation of almost 23 percent (note that the definition of Nu_Z includes the nanofluid thermal conductivity that, as we know, also increases with the parameter φ).

3.2 Effect of parameters Re and φ on turbulent heat transfer

The above beneficial effect due to the presence of nanoparticles has also been clearly shown in Figure 4(a) and (b) that shows, respectively, the variation of the fully developed wall heat transfer coefficient h_{fd} (W/m^{2}K) and the nanofluid-to-base fluid heat transfer coefficients ratio $(h_{fd})_r$ with respect to the key parameters φ and Re. As one may expect, both of these parameters have important influence on the heat transfer. Thus, for a given value of Reynolds number, heat transfer coefficient clearly augments with an increase of particle loading parameter φ; for $Re = 10^4$, for example, the heat transfer coefficient has increases from 8,808 W/m^{2}K at $\varphi = 0$ percent to 13,190 W/m^{2}K at $\varphi = 10$ percent. On the other hand, for a fixed particle volume concentration, say $\varphi = 5$ percent, for example, h_{fd} has increased from 10,837 W/m^{2}K to a value as high as 180,482 W/m^{2}K for Re augmenting from 10^4 to 5×10^5. It is very interesting to observe from Figure 4(a) that a combination of high particle loading and high Reynolds number flow can produce a rather high wall heat transfer rate, which appears very useful for some advanced and special thermal applications. The heat transfer enhancement with respect to the base fluid (saturated water) is represented by the ratio of fully developed heat transfer coefficients, $(h_{fd})_r$ (Figure 4(b)). Again, the heat transfer advantage of nanofluids over the base fluid is obvious as we can observe that the ratio $(h_{fd})_r$ considerably increases with the augmentation of the parameter φ. Thus,

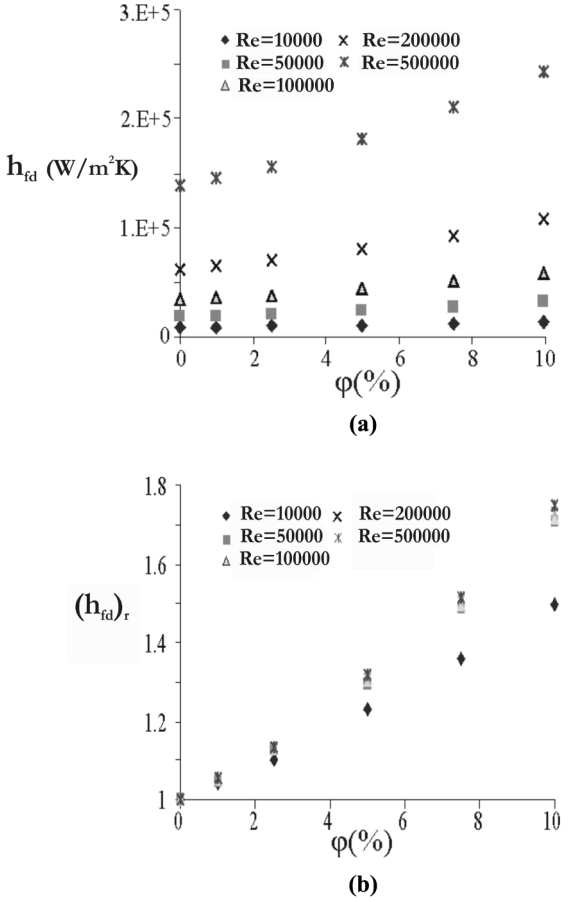

Figure 4.
Effect of parameters φ and *Re* on: (a) fully developed heat transfer coefficient; and (b) ratio of fully developed heat transfer coefficients

for $Re = 10^4$ in particular, such a heat transfer enhancement is estimated to be 5, 10, 23, 35 and 50 percent, respectively, for $\varphi = 1$, 2.5, 5, 7.5 and 10 percent. One can also observe that for sufficiently high Reynolds numbers, say for $Re \geq 5 \times 10^4$, the influence of this parameter *Re* on the heat transfer coefficient ratio $(h_{fd})_r$ tends to become negligible.

It is very interesting to mention that the above behaviors and trends regarding the increase of heat transfer as function of the parameters φ and *Re* have been found to be consistent with experimental data by Pak and Cho (1998) and Li and Xuan (2002). Table I shows, in particular, the comparison between our results as obtained for the ratio $(h_{fd})_r$ and the case $Re = 50{,}000$ and the corresponding values obtained by using the only and recent experimental correlation proposed by Pak and Cho (1998) for a turbulent flow of nanofluids. One can see that the agreement appears quite satisfactory with relative errors estimated to be 9, 12 and 14 percent, respectively, for $\varphi = 1$, 2.5 and 5 percent (it should be noted that Pak and Cho (1998) correlation is applicable, in principle, to a maximum particle volume fraction of nearly 3.2 percent; hence the comparison shown for the case of 5 percent of volume concentration is only

for indicating the trend). Such a comparison may give a certain indication about the appropriateness as well as the reliability of both the mathematical model and the turbulent model used in the present study. Furthermore, one may also state, although indirectly, that the assumption regarding the approximation of a nanofluid as a single-phase homogenous fluid appears reasonable.

Figure 5 shows the variation of the corresponding fully developed Nusselt number as function of parameters Re and φ. As one may expect from the previous discussion concerning the nanofluid heat transfer behavior, it is observed that the Nusselt number increases considerably with both of these parameters. Thus, for a given Reynolds number, say $Re = 10^4$, Nu_{fd} increases in fact from 145 ($\varphi = 0$ percent) to 165 ($\varphi = 10$ percent); on the other hand, for a fixed particle volume fraction, say $\varphi = 5$ percent, for example, Nusselt number has passed from 156 to a value as high as 2,630 for Re augmenting from 10^4 to 5×10^5. It should be noted that in Figure 5, the increase of Nu_{fd} with respect to parameter φ appears less pronounced for low and moderate Reynolds numbers, which is due to the fact that the definition of Nu_{fd} includes nanofluid thermal conductivity that also increases with particle volume concentration. Again, one can observe that a combination of both high Reynolds number and high particle concentration may lead to a rather interestingly high value of the Nusselt number.

We have attempted to see whether our numerical results for Nusselt number as obtained from the simulations can be represented either by Dittus and Boelter (1930) and Pak and Cho (1998) correlations. Note that the first correlation is well known for

Particle loading φ (percent)	$(h_{fd})_r$ present study	$(h_{fd})_r$ by correlation from Pak and Cho (1998)[a]
1	1.05	1.16
2.5	1.12	1.27
5[b]	1.30	1.51

Notes: [a]Pak and Cho (1998) data are limited to a maximum particle volume concentration of 3.16 percent; [b]for indication of the trend only

Table I.
Comparison with experimental correlation for ratio $(h_{fd})_r$, $Re = 5 \times 10^4$

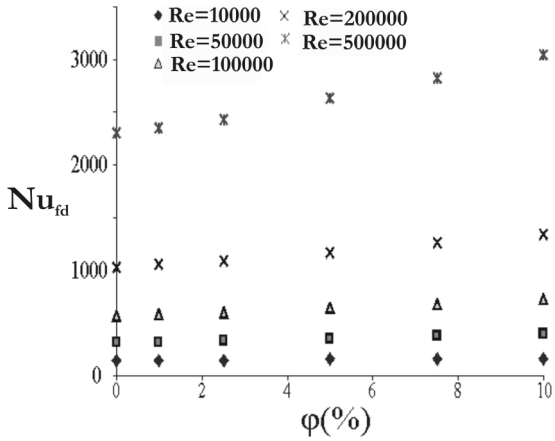

Figure 5.
Effect of parameters φ and Re on fully developed Nusselt number

computing Nusselt number for a turbulent flow while the second one, also empirical, was likely the first that has been proposed based on data collected from various types of nanofluid. The outcome of such a process was somewhat little deceiving. First, by comparing our results for Nusselt number to the values as given by the Dittus and Boelter correlation using corresponding values of nanofluid parameters Re and Pr, we have found that the maximum, mean and standard deviation of the relative error are, respectively, 46, 18 and 13 percent. We have also observed that in general, errors remain relatively acceptable and vary from 5 to 22 percent for $Re \geq 5 \times 10^4$; while for the case $Re = 10^4$, however, drastically large errors ranging from 37 to 46 percent have been found. Nevertheless, we believe that except of a low Reynolds number, in particular $Re = 10^4$, the Dittus and Boelter (1930) correlation may be approximately considered for calculating the nanofluid heat transfer for turbulent tube flows. Following the same idea, this seems to indicate that the assumption of the single-phase fluid to representing a nanofluid appears, to our opinion, to be reasonable for the studied case and ranges of the governing parameters considered.

Regarding the Pak and Cho (1998) experimental correlation – say the only available correlation that can be, in principle, used for the type of nanofluid under study – we have first attempted to see whether such correlation can be used over the entire ranges of the governing parameters considered. Such an attempt was unfortunately unsuccessful! The following errors were encountered: 40, 13 and 13 percent, respectively, as maximum, mean and standard deviation of the relative error. We have also observed that the deviations remain slightly less pronounced than those found with the Dittus and Boelter (1930) correlation. For example, the relative errors are ranging from 1 to 16 percent for the range $Re \geq 5 \times 10^4$; again, for the cases $Re = 10^4$ in particular, large relative errors to a maximum of 40 percent have been found. Hence, we can also say that the Pak and Cho (1998) correlation appears appropriate for representing numerical results for the range $Re \geq 5 \times 10^4$. The possible reason for such large discrepancies may come from the fact that, as it has been mentioned previously, Pak and Cho (1998) experimental data were limited to relatively low particle concentration, say $\varphi \leq 3.2$ percent, and flow Reynolds number ranging from 10^4 to 10^5. As a second attempt, we have employed Pak and Cho (1998) correlation only for the ranges $Re \leq 10^5$ and $\varphi \leq 2.5$ percent, say within the ranges of the parameters originally considered by these authors. As one can expect, the discrepancies appear much lower, with an exception again for the cases with $Re = 10^4$ for which a maximum relative error of 40 percent has been found. Fortunately, for all other values of $Re \leq 10^5$ (and $\varphi \leq 2.5$ percent), the relative errors remain low and vary from 1 to 3 percent, which appear rather satisfactory. Complete details and discussion regarding the performance of the above correlations were presented in Maïga (2004).

In conjunction with the above discussion, we attempted in this study to provide a new correlation that would cover larger range of the parameters Re and φ. The following correlation was obtained from the numerical results using an available genetic algorithm (Turkkan, 2004):

$$Nu_{\mathrm{fd}} = 0.085\, Re^{0.71}\, Pr^{0.35} \tag{12}$$

This correlation exhibits maximum, mean and standard deviation of relative error of 19, 12 and 6 percent, which appear, by far, more reasonable. It is expected to be

applicable for the following ranges of the parameters: *Re* from 10^4 to 5×10^5, *Pr* from 6.6 to 13.9 and φ from 0 to 10 percent.

3.3 Effect of parameters Re *and* φ *on wall shear stress*

The above beneficial influence due to the presence of nanoparticles on heat transfer performance has, unfortunately, a somewhat major drawback on the wall shear stress. In fact, it has been observed that for laminar flow regime, nanofluids produce higher wall friction than a base fluid for different confined flow geometries (Maïga *et al.* 2005; Roy *et al.* 2004). Similar trends were also noticed regarding the turbulent flow regime considered in this study. Figure 6(a) and (b) shows, respectively, the variation of the fully developed wall shear stress τ_{fd} (Pa) and its nanofluid-to-base fluid ratio $(\tau_{fd})_r$ as function of the parameters *Re* and φ. One can see that, in general, the wall friction increases considerably with an increase of both parameters. Thus, for given Reynolds number, τ_{fd} increases with respect to the particle loading parameter φ; this effect appears clearly more pronounced for high Reynolds numbers. Thus, for $Re = 2 \times 10^5$ in particular,

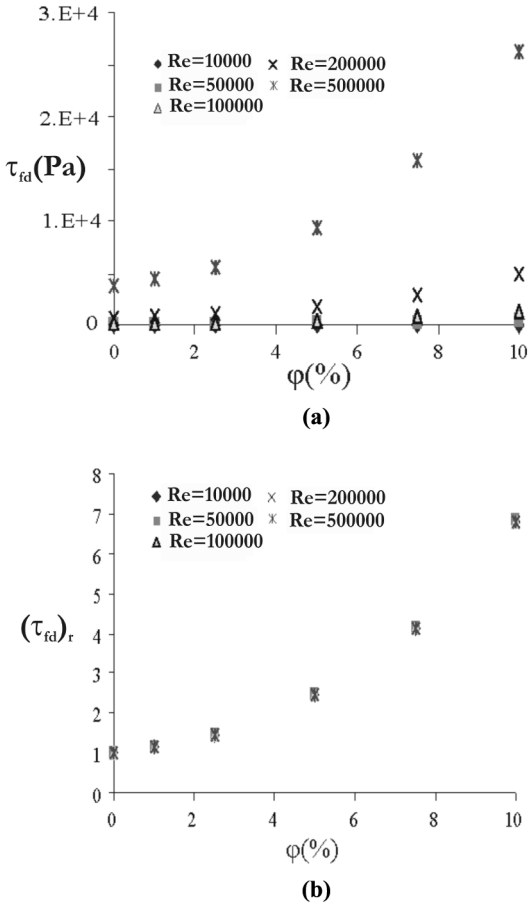

Figure 6.
Effect of parameters φ and *Re* on: (a) fully developed wall shear stress; and (b) ratio of fully developed wall friction

values of τ_{fd} are, respectively, 728 Pa ($\varphi = 0$) and 4,960 Pa ($\varphi = 10$ percent). It should be mentioned that due to an extended scale of τ_{fd}, its increase with respect to φ appears "graphically" less important for relatively low Reynolds numbers, say for $Re \leq 10^5$. In reality, τ_{fd} always augments with φ regardless the values of Re; for $Re = 5 \times 10^4$, for example, τ_{fd} has in fact increased from 61 to 418 Pa as φ augments from 0 to 10 percent. Such a behavior is obviously due to the increase of fluid dynamic viscosity that also augments considerably with an increase of particle loading. On the other hand, the corresponding increase of the wall shear stress with respect to the flow Reynolds number is, as one may expect, very important. For $\varphi = 2.5$ percent, for example, τ_{fd} has augmented from 10 Pa to nearly 5,635 Pa for Re increasing from 10^4 to 5×10^5. At a higher value of φ, the effect due to the Reynolds number even becomes more pronounced.

On the relative nanofluid-to-base fluid basis, it has been found that the ratio $(\tau_{fd})_r$ also increases considerably with the particle loading parameter φ (Figure 6(b)). It is very interesting to observe that the influence of parameter Re on the ratio $(\tau_{fd})_r$ appears practically negligible; for a given particle concentration, $(\tau_{fd})_r$ is almost identical for all of the Reynolds numbers considered. From this figure, $(\tau_{fd})_r$ has as values, 1.15, 1.47, 2.45, 4.11 and 6.81, respectively, for $\varphi = 1$, 2.5, 5, 7.5 and 10 percent. This implies that, for 10 percent particle concentration in particular, one would expect a wall shear stress of factor nearly seven times of that of saturated water, given identical flow Reynolds number. Such a drastic effect on the wall shear stress may, of course, constitute a major drawback regarding some potential applications of the nanofluids.

4. Conclusion

In this paper, we have investigated, by numerical simulations, the thermal performance of a nanofluid, water-γAl_2O_3 mixture, which flows under turbulent regime inside a uniformly heated tube. Results have clearly shown that with the presence of nanoparticles, heat transfer of a resulting nanofluid has, by far, considerably increased while compared to that of saturated water. Such an enhancement has been found to become more pronounced with the increase of the particle volume concentration as well as with the flow Reynolds number. A particularly important wall heat transfer rate may be achieved by combining a high particle loading and mass flow rate. In reverse, it is observed that nanofluids exhibit, in general, more important wall shear stress than that of the base fluid; such an increase also becomes mores pronounced with the particle volume concentration. A new correlation, $Nu_{fd} = 0.085\, Re^{0.71}\, Pr^{0.35}$, has been obtained from the parametric study in order to compute the fully-developed heat transfer coefficient as function of the flow Reynolds number and the fluid Prandtl number; such correlation is valid for $10^4 \leq Re \leq 5 \times 10^5$, $6.6 \leq Pr \leq 13.9$ and $0 \leq \varphi \leq 10$ percent.

References

Anderson, D.A., Tannehill, J.C. and Pletcher, R.H. (1984), *Computational Fluid Mechanics and Heat Transfer*, Hemisphere Pub. Co., New York, NY.

Choi, S.U-S. (1995), *Enhancing Thermal Conductivity of Fluids with Nanoparticles*, ASME Publications, New York, NY, FED-Vol. 231/MD-Vol. 66, pp. 99-105.

Das, S.K., Putra, N., Thiesen, P. and Roetzel, W. (2003), "Temperature dependence of thermal conductivity enhancement for nanofluids", *J. Heat Transfer*, Vol. 125, pp. 567-74.

Dittus, F.W. and Boelter, L.M.K. (1930), *Engineering*, Vol. 2, p. 443.

Drew, D.A. and Passman, S.L. (1999), *Theory of Multicomponent Fluids*, Springer, Berlin.

Eastman, J.A., Choi, S.U-S., Li, S., Soyez, G., Thompson, L.J. and DiMelfi, R.J. (1999), "Novel thermal properties of nanostructured materials", *J. Metastable Nanocrystalline Materials*, Vol. 2 No. 6, pp. 629-34.

Eastman, J.A., Choi, S.U-S., Li, S., Yu, W. and Thompson, L.J. (2001), "Anomalously increase effective thermal conductivities of ethylene glycol-based nanofluids containing copper nanoparticles", *Appl. Phys. Lett.*, Vol. 78 No. 6, pp. 718-20.

Hamilton, R.L. and Crosser, O.K. (1962), "Thermal conductivity of heterogeneous two-component systems", *I & EC Fundamentals*, Vol. 1 No. 3, pp. 187-91.

Keblinski, P., Eastman, J.A. and Cahill, D.G. (2005), "Nanofluids for thermal transport", *Materialstoday*, pp. 36-44, June.

Keblinski, P., Phillpot, S.R., Choi, S.U-S. and Eastman, J.A. (2002), "Mechanisms of heat flow in suspensions of nano-sized particles (nanofluids)", *Int. J. Heat Mass Transfer*, Vol. 45, pp. 855-63.

Launder, B.E. and Spalding, D.B. (1972), *Mathematical Models of Turbulence*, Academic Press, New York, NY.

Launder, B.E. and Spalding, D.B. (1974), "The numerical computation of turbulent flows", *Computer Methods in Applied Mechanics and Engineering*, Vol. 3, pp. 269-89.

Lee, S. and Choi, S.U-S. (1996), *Application of Metallic Nanoparticle Suspensions in Advanced Cooling Systems*, ASME Publications, New York, NY, pp. 227-34, PVP-Vol. 342/MD-Vol. 72.

Lee, S., Choi, S.U-S., Li, S. and Eastman, J.A. (1999), "Measuring thermal conductivity of fluids containing oxide nanoparticles", *J. Heat Transfer*, Vol. 121, pp. 280-9.

Li, Q. and Xuan, Y. (2002), "Convective heat transfer performances of fluids with nano-particles", *Proceedings of the 12th Int. Heat Transfer Conference, Grenoble, France*, pp. 483-8.

Maïga, S.E.B. (2004), "Forced convection of nanofluids in a uniformly heated tube/convection forcée dans un tuyau chauffé uniformément utilisant des nanofluides", Master's thesis, Faculty of Engineering, Université de Moncton, Moncton.

Maïga, S.E.B., Nguyen, C.T., Galanis, N. and Roy, G. (2004), "Heat transfer enhancement in forced convection laminar tube flow by using nanofluids", paper CHT-04-101, *Proceedings of the CHT-04/ICHMT International Symposium on Advances in Computational Heat Transfer III*, p. 24.

Maïga, S.E.B., Palm, S.J., Nguyen, C.T., Roy, G. and Galanis, N. (2005), "Heat transfer enhancement by using nanofluids in forced convection flows", *Int. J. Heat Fluid Flow*, Vol. 26, pp. 530-46.

Masuda, H., Ebata, A., Teramae, K. and Hishinuma, N. (1993), "Alteration of thermal conductivity and viscosity of liquid by dispersing ultra-fine particles (dispersion of γ-Al_2O_3, SiO_2 and TiO_2 ultra-fine particles)", *Netsu Bussei*, Vol. 4 No. 4, pp. 227-33 (in Japanese).

Ohara, T. and Suzuki, D. (2000), "Intermolecular energy transfer at a solid-liquid interface", *Microscale Thermophysics Engineering*, Vol. 4, pp. 189-96.

Pak, B.C. and Cho, Y.I. (1998), "Hydrodynamic and heat transfer study of dispersed fluids with submicron metallic oxide particles", *Experimental Heat Transfer*, Vol. 11 No. 2, pp. 151-70.

Patankar, S.V. (1980), *Numerical Heat Transfer and Fluid Flow*, Hemisphere Inc./McGraw-Hill, New York, NY.

Putra, N., Roetzel, W. and Das, S.K. (2003), "Natural convection of nanofluids", *Heat and Mass Transfer*, Vol. 39, pp. 775-84.

Roy, G., Nguyen, C.T. and Lajoie, P-R. (2004), "Numerical investigation of laminar flow and heat transfer in a radial flow cooling system with the use of nanofluids", *Superlattices and Microstructures*, Vol. 35 Nos 3-6, pp. 497-511.

Turkkan, N. (2004), *Real Coded Genetic Algorithm for Minimization Problems*, Faculty of Engineering, Université de Moncton, Moncton, Vol. 3.01, available at: www.umoncton.ca/Turk/Genetik201.xls

Wang, X., Xu, X. and Choi, S.U-S. (1999), "Thermal conductivity of nanoparticles-fluid mixture", *J. Thermophysics and Heat Transfer*, Vol. 13 No. 4, pp. 474-80.

Wang, B-X., Zhou, L-P. and Peng, X-F. (2003), "A fractal model for predicting the effective thermal conductivity of liquid with suspension of nanoparticles", *Int. J. Heat Mass Transfer*, Vol. 46, pp. 2665-72.

Warsi, Z.U.A. (1999), *Fluid Dynamics Theoretical and Computational Approaches*, 2nd ed., CRC Press, Boca Raton, FL.

Wen, D. and Ding, Y. (2004), "Experimental investigation into convective heat transfer of nanofluids at the entrance region under laminar flow conditions", *Int. J. Heat Mass Transfer*, Vol. 47, pp. 5181-8.

Xuan, Y. and Li, Q. (2000), "Heat transfer enhancement of nanofluids", *Int. J. Heat Fluid Flow*, Vol. 21, pp. 58-64.

Xuan, Y. and Roetzel, W. (2000), "Conceptions for heat transfer correlation of nanofluids", *Int. J. Heat Mass Transfer*, Vol. 43, pp. 3701-7.

Xuan, Y., Li, Q. and Hu, W. (2003), "Aggregation structure and thermal conductivity of nanofluids", *AIChE J.*, Vol. 49 No. 4, pp. 1038-43.

Yang, Y., Zhang, Z.G., Grulke, E.A., Anderson, W.B. and Wu, G. (2005), "Heat transfer properties of nanoparticle-in-fluid dispersions (nanofluids) in laminar flow", *Int. J. Heat Mass Transfer*, Vol. 48 No. 6, pp. 1107-16.

Yuan, S.W. (1967), *Foundations of Fluid Mechanics*, Prentice-Hall, Englewood Cliffs, NJ.

Corresponding author
Cong Tam Nguyen can be contacted at: nguyenc@umoncton.ca